

Centroid Approximation for Bootstrap

Mao Ye, Qiang Liu
University of Texas at Austin
{my21, lqiang}@cs.utexas.edu

Abstract

Bootstrap is a principled and powerful frequentist statistical tool for uncertainty quantification. Unfortunately, standard bootstrap methods are computationally intensive due to the need of drawing a large i.i.d. bootstrap sample to approximate the ideal bootstrap distribution; this largely hinders their application in large-scale machine learning, especially deep learning problems. In this work, we propose an efficient method to explicitly *optimize* a small set of high quality “centroid” points to better approximate the ideal bootstrap distribution. We achieve this by minimizing a simple objective function that is asymptotically equivalent to the Wasserstein distance to the ideal bootstrap distribution. This allows us to provide an accurate estimation of uncertainty with a small number of bootstrap centroids, outperforming the naive i.i.d. sampling approach. Empirically, we show that our method can boost the performance of bootstrap in a variety of applications.

1 Introduction

Bootstrap is a simple and principled frequentist uncertainty quantification tool and can be flexibly applied to obtain data uncertainty estimation with strong theoretical guarantees (Hall et al., 1988; Austern and Syrkanis, 2020; Chatterjee et al., 2005; Cheng et al., 2010). In particular, when combined with the maximum likelihood estimator or more general M-estimators, bootstrap provides a general-purpose, plug-and-play non-parametric inference framework for general probabilistic models without case-by-case derivations; this makes it a promising frequentist alternative to Bayesian inference.

However, the standard bootstrap inference is highly expensive in both computation and memory as it typically requires drawing a large number¹ of i.i.d. bootstrap particles (samples) to obtain an accurate uncertainty estimation. With a small number of particles, bootstrap may perform poorly. As a consequence, when applied to deep learning, we need to store a large number of neural networks and feed the input into a tremendous number of networks every time we make inference, which

¹For example, thousands of, as suggested by Statistics textbooks such as Wasserman (2013).

can be quite expensive and even unaffordable for deep learning problems with huge models². For example, in autonomous driving applications, our device can only store a limited number of models and we need to make decisions within a short time, which makes the standard bootstrap with a large number of models no more feasible. Typical ensemble methods in deep learning, such as Lakshminarayanan et al. (2016); Huang et al. (2017); Vyas et al. (2018); Maddox et al. (2019); Liu and Wang (2016), can only afford to use a small number (e.g., less than 20) of models.

Therefore, to make bootstrap more accessible in modern machine learning, it is essential to develop new approaches that break the key computation and memory barriers mentioned above. We are thus motivated to consider the following problem:

How to improve the accuracy of bootstrap inference when the number of particles is limited?

We attack this challenge by presenting an efficient centroid approximation for bootstrap. Our method replaces the i.i.d. bootstrap particles with a set of carefully optimized *centroid particles* that are guaranteed to provide an accurate and compact approximation to the ideal bootstrap distribution so that only a smaller number of particles is needed to obtain good performance.

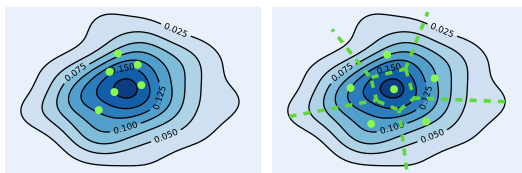


Figure 1: The solid lines represent the density of the target distribution. Left figure: Typical i.i.d. particles that are randomly distributed on the domain. Right figure: The learned diversified centroids that are well distributed on the domain. The centroids partition the domain into several disjoint regions (separated by the dashed lines in the figure) and each centroid can be viewed as the ‘K-means’ center of the region it belongs to.

Our method is based on minimizing a specially designed objective function that is asymptotically equivalent to the Wasserstein distance between the ideal bootstrap distribution and the particle distribution formed by the learned centroids. During the training, each centroid adjusts its location being aware of the locations of the others so that centroids are diversified and well distributed on the domain. Our method is similar to doing K-means on the ideal bootstrap distribution, finding K representative centroids that well represent K separate parts of the target distribution’s domain in an optimal way. As centroids are optimized to better approximate the distribution, our approach naturally improves over the vanilla bootstrap with i.i.d. particles. See Figure 1 for illustration.

Empirically, we apply the centroid approximation method to various applications, including confidence interval estimation (DiCiccio et al., 1996), bootstrap method for contextual bandit (Riquelme et al., 2018), bootstrap deep Q-network (Osband et al., 2016) and bagging method (Breiman, 1996) for neural networks. We find that our method consistently improves over the standard bootstrap.

²While training cost is an extra burden, it is small compared with the cost of making prediction as we only need to train the model once but make countless predictions at deployment.

Notation We use $\|\cdot\|$ to represent the ℓ_2 norm for a vector and the operator norm for a matrix. We denote the integer set $\{1, 2, \dots, N\}$ by $[N]$. Given any m , we define the probability simplex $\mathcal{C}^m := \{[v_1, \dots, v_m] \in \mathbb{R}^m : v_i \geq 0, \forall i \in [m] \text{ and } \sum_{i \in [m]} v_i = 1\}$. For a symmetric matrix M , we denote its minimal eigenvalue by $\lambda_{\min}(M)$. For a positive-definite matrix M , if $M = A^\top A$, then we denote A by $M^{1/2}$. We denote the Wasserstein distance between two distribution ρ_1 and ρ_2 by $\mathcal{W}_2[\rho_1, \rho_2]$. We use O and o to denote the conventional big-O and small-o notation and use O_p to denote the stochastic boundedness. We use \xrightarrow{d} to denote convergence in distribution.

2 Background

Suppose we have a model f_θ parameterized by θ in a parameter space $\Theta \subseteq \mathbb{R}^d$. Let $\{x_i\}_{i=1}^n \subset \mathcal{X}$ be a training set with n data points on \mathcal{X} . Assume $\ell(x, f_\theta)$ is the negative log-likelihood of data point x with model f_θ . A standard approach to estimate θ is maximum likelihood estimator (MLE), which minimizes the negative log-likelihood function (loss) over the training set

$$\hat{\theta} = \arg \min_{\theta \in \Theta} \mathcal{L}(\theta), \quad \mathcal{L}(\theta) = \sum_{i=1}^n \ell(x_i, f_\theta)/n.$$

Here the MLE $\hat{\theta}$ provides a point estimation without any information on the data uncertainty. Bootstrap is a simple and effective frequentist method to quantify the uncertainty. The bootstrap loss is a randomly perturbed loss defined as

$$\mathcal{L}_{\mathbf{w}}(\theta) = \sum_{i=1}^n w_i \ell(x_i, f_\theta)/n,$$

where $\mathbf{w} = [w_1, \dots, w_n]^\top$ is a set of random weights of data points drawn from some distribution π . A typical choice of π is the multinomial distribution with uniform probability, which corresponds to resampling on the training set with replacement. Given \mathbf{w} , one can calculate its associated bootstrap particle by minimizing the bootstrap loss:

$$\hat{\theta}_{\mathbf{w}} = \arg \min_{\theta \in \Theta} \mathcal{L}_{\mathbf{w}}(\theta). \tag{1}$$

Let ρ_π be the distribution of $\hat{\theta}_{\mathbf{w}}$ when $\mathbf{w} \sim \pi$. Bootstrap theory indicates that we can quantify the data uncertainty of θ or any function $g(\theta)$ using ρ_π . We call ρ_π the ideal bootstrap distribution and it is the main object we want to approximate.

Denote δ_θ as the delta measure centered at θ . Standard bootstrap method approximates ρ_π by the particle distribution $\hat{\rho}_\pi(\cdot) = \sum_{j=1}^m \delta_{\hat{\theta}_{\mathbf{w}_j}}(\cdot)/m$ formed by m i.i.d. particles $\{\hat{\theta}_{\mathbf{w}_j}\}_{j=1}^m$, which can be obtained by drawing m i.i.d. weights $\{\mathbf{w}_j\}_{j=1}^m$ from π and calculating each $\hat{\theta}_{\mathbf{w}_j}$ based on (1). However, for deep learning applications, as discussed in the introduction, storing and making inference using a large number m of bootstrap particles can be quite expensive. On the other hand, if m is small, $\hat{\rho}_\pi$ tends to be a poor approximation of ρ_π . In this paper, we aim to improve the approximation of the particle distribution when m is small.

3 Method

Our idea is simple. Instead of using i.i.d. particles, in which the location of each particle is independent from that of the others, we try to actively optimize the location of each particle so that particles are diversified, better distributed and eventually providing a particle distribution with improved approximation accuracy. A natural way to achieve this goal is to explicitly optimize a set of points $\{\theta_j\}_{j=1}^m$ (called centroids) jointly such that the Wasserstein distance between ρ_π and the induced particle distribution is minimized:

$$\{\theta_j^*, v_j^*\}_{j=1}^m = \arg \min_{\theta_1, \dots, \theta_m \in \Theta, [v_1, \dots, v_m] \in \mathcal{C}^m} \mathcal{W}_2 \left[\sum_{j=1}^m v_j \delta_{\theta_j}, \rho_\pi \right]. \quad (2)$$

Here we consider a Wasserstein distance \mathcal{W}_2 equipped with a special data-dependent distance metric $\|\cdot\|_D$ that will be introduced later in (5). We note that here we also optimize the probability weights $\{v_j\}_{j=1}^m$ of the centroids. Finding the optimal centroids and probability weights can be decomposed into two steps: the centroid learning phase and the probability weights learning phase, based on the facts in (3,4).

$$\mathcal{W}_2^2 \left[\sum_{j \in [m]} v_j^* \delta_{\theta_j^*}, \rho_\pi \right] = J_\pi(\{\theta_j^*\}_{j=1}^m), \text{ where } J_\pi(\{\theta_j\}_{j=1}^m) := \mathbb{E}_{\mathbf{w} \sim \pi} \left[\min_{j \in [m]} \|\theta_j - \hat{\theta}_{\mathbf{w}}\|_D^2 \right]. \quad (3)$$

Here (3) implies that, to find the optimal particle distribution in (2), we can start with the centroid learning phase where we only need to optimize the centroids. It can be achieved by minimizing $J_\pi(\{\theta_j\}_{j=1}^m)$, which is the averaged distance of bootstrap particles to their closest centroid. After we obtain the optimal centroids, the optimal probability weights can be learned by (4):

$$v_j^* = \tilde{v}_j^* / \sum_{s \in [m]} \tilde{v}_s^*, \text{ where } \tilde{v}_j^* = \mathbb{P}_{\mathbf{w} \sim \pi} \left(j = \arg \min_{j \in [m]} \|\theta_j^* - \hat{\theta}_{\mathbf{w}}\|_D^2 \right). \quad (4)$$

Here v_j^* is the proportion of bootstrap particles that are closest to the centroid j . We emphasize that the optimal solution to two-stage learning is guaranteed to be the global minimizer of the loss in (2).

However, the key issue is that the losses in both (2, 3) can not be computed in practice, as they require us to access ρ_π (i.e., obtain $\hat{\theta}_{\mathbf{w}}$ first in order to calculate the loss). To handle this issue, we seek an easy-to-compute surrogate loss. Our idea is based on the following observation. Assuming the size of training data is large, which is usually the case in deep learning, we can expect that $\theta_{\mathbf{w}}$ will be centered around a small region³. It implies that we should search the centroid in this small region. Notice that when θ is close to $\hat{\theta}_{\mathbf{w}}$, based on Taylor approximation, we have

$$\begin{aligned} \mathcal{L}_{\mathbf{w}}(\theta) &\approx \mathcal{L}_{\mathbf{w}}(\hat{\theta}_{\mathbf{w}}) + \nabla_{\theta}^{\top} \mathcal{L}_{\mathbf{w}}(\hat{\theta}_{\mathbf{w}})(\theta - \hat{\theta}_{\mathbf{w}}) + 1/2(\theta - \hat{\theta}_{\mathbf{w}})^{\top} \nabla_{\theta}^2 \mathcal{L}_{\mathbf{w}}(\hat{\theta}_{\mathbf{w}})(\theta - \hat{\theta}_{\mathbf{w}}) \\ &\approx \mathcal{L}_{\infty}(\theta_0) + 1/2\|\theta - \hat{\theta}_{\mathbf{w}}\|_D^2, \text{ where } \|V\|_D^2 := V^{\top} \nabla_{\theta}^2 \mathcal{L}_{\infty}(\theta_0) V. \end{aligned} \quad (5)$$

³This can be formally characterized by central limit theorem as discussed in Section 4.

Here $\mathcal{L}_\infty(\theta) := \mathbb{E}_x \ell(x, f_\theta)$ denotes the population loss; θ_0 is the minimizer of $\mathcal{L}_\infty(\theta)$. In (5), we use the facts⁴ that $\nabla_\theta^\top \mathcal{L}_w(\hat{\theta}_w) = 0$; and with large training set, $\hat{\theta}_w \approx \theta_0$, $\mathcal{L}_w(\cdot) \approx \mathcal{L}_\infty(\cdot)$ and $\nabla_\theta^2 \mathcal{L}_w(\cdot) \approx \nabla_\theta^2 \mathcal{L}_\infty(\cdot)$. Since $\mathcal{L}_\infty(\theta_0)$ is some (unknown) constant independent with θ , we can replace the $\|\theta_j - \hat{\theta}_w\|_D^2$ in (3) by $\mathcal{L}_w(\theta_j)$ as it only adds some constant into the loss.

Intuitively, we can expect that the centroid closest to $\hat{\theta}_w$ is the one that gives the smallest loss on \mathcal{L}_w . It motivates us to learn the centroids via the modified centroid learning phase:

$$\{\theta_j^*\}_{j=1}^m = \arg \min_{\theta_1, \dots, \theta_m \in \Theta} \mathbb{E}_{w \sim \pi} [\min_{j \in [m]} \mathcal{L}_w(\theta_j)]. \quad (6)$$

Similarly, the optimal probability weights can be learned via the modified weight learning phase:

$$v_j^* = \tilde{v}_j^* / \sum_{s \in [m]} \tilde{v}_s^*, \text{ where } \tilde{v}_j^* = \mathbb{P}_{w \sim \pi} (j \in \arg \min_{j \in [m]} \mathcal{L}_w(\theta_j^*)). \quad (7)$$

We note that here we slightly abuse the notation of θ_j^* and v_j^* in (3,4) and (6,7) for simplification. In the later context, θ_j^* and v_j^* are used based on their definitions in (6,7).

Connection to K-means By viewing the target distribution as a set of particles that we want to cluster, in K-means clustering, each centroid (i.e., K-means center) represents one of the K disjoint groups⁵ of particles, which is formed by assigning each particle in the whole set to the closest centroid among all the K centroids. K-means learns the optimal K centroids in the way that they can best approximate the whole set. The ‘closeness’ for assigning the particles is measured by the distance between the two points. As pointed out by [Canas and Rosasco \(2012\)](#), K-means essentially searches the optimal particle distribution formed by the K centroids that minimizes its Wasserstein distance to the target distribution. Our centroid approximation idea follows the same fashion of clustering but measures the ‘closeness’ by examining the bootstrap loss of the centroids so that we can still learn the optimal centroids without obtaining the i.i.d. bootstrap particles first. We also point out that, while we share the same objective as K-means, the optimization algorithms differ. The Expectation-Maximization type of algorithm used by K-means is not applicable to our scenario.

3.1 Training

The optimization of (6) can be solved by gradient descent. Suppose $\theta_j^*(t)$ is the j -th centroid at iteration t . We initialize $\{\theta_j^*(0)\}_{j=1}^m$ by sampling from ρ_π and at iteration t , we update θ_j^* by applying the gradient descent on the loss in (6), which yields

$$\begin{aligned} \theta_j^*(t+1) &\leftarrow \theta_j^*(t) - \epsilon_t g(\theta_j^*(t)), \\ g(\theta_j^*(t)) &= \nabla_\theta \mathbb{E}_{w \sim \pi} [\mathbb{I}\{j \in u_w(t)\} \mathcal{L}_w(\theta_j^*(t))] / v_j^*(t), \end{aligned} \quad (8)$$

where we define the index of the closest centroid to particle $\hat{\theta}_w$ as $u_w(t) = \arg \min_{j \in [m]} \mathcal{L}_w(\theta_j^*(t))$ and $v_j^*(t) = \mathbb{P}_{w \sim \pi} (j \in u_w(t))$ denotes the probability that centroid j is the one that gives the

⁴We defer the detailed analysis to Section 4.

⁵i.e. the regions separated by the dashed lines in the right plot of Figure 1.

lowest bootstrap loss. The denominator $v_j^*(t)$ in $g(\theta_j^*(t))$ is optional. However, notice that the magnitude of numerator in $g(\theta_k^*(t))$ decays with larger m , which might require an adjustment of the learning rate when m changes. This adjustment can be avoided by rescaling with $v_k^*(t)$.

We note that $\{\theta_j^*(0)\}_{j=1}^m$ is just m i.i.d. bootstrap particles which is not optimal for approximation and our algorithm can be viewed as an approach for refining the m particles by solving (6). In practice, we find that we can simply use random initialization (e.g., draw θ from some Gaussian distribution) instead.

Centroid Degeneration Phenomenon Naively applying the updating rule (8) may cause a degeneration phenomenon: When a centroid happens to give considerably worse performance than others, which can be caused by the stochasticity of gradient or worse initialization, the performance of this centroid will remain considerably worse throughout the optimization. The reason is simple. As this centroid (e.g. $\theta_j^*(t)$) gives a considerably worse performance, the probability that it gives the lowest bootstrap loss, i.e., $v_j^*(t)$, is small. As a consequence, the gradient that updates this centroid is only based on aggregating information from a small low-density region of π and hence can be unstable and further degrades this centroid. Note that this mechanism is self-reinforced since when this centroid cannot be effectively improved in the current iteration, it faces the same issue in the next one. As a result, this centroid is always significantly worse than the others.

We call this undesirable phenomenon *centroid degeneration* and we want to prevent this phenomenon because when it happens, we have a centroid that is not representative and contributes less to approximating ρ_π . We solve this issue with a simple solution and here is the intuition. The reason that a centroid degenerates lies in that this centroid is far from the good region where it gives a good performance. And when this happens, we should push the centroid to move towards this good region, which can be achieved by using the common gradient over the whole training data. Specifically, we define a threshold γ , indicating centroid j is degenerated if $v_j^*(t) \leq \gamma$. And when it happens, we update using the common gradient over the whole data:

$$\theta_j^*(t+1) \leftarrow \theta_j^*(t) - \epsilon_t \nabla_\theta \mathcal{L}(\theta_j^*(t)). \quad (9)$$

In section 4, we give a theoretical analysis on why this modification is important and is able to solve the centroid degeneration issue.

Practical Algorithm In practice, we estimate the gradient by replacing the expectation over $w \sim \pi$ in (8) with averaging over M i.i.d. samples $\{w_h\}_{h=1}^M$ drawn from π :

$$\hat{g}(\theta_j^*(t)) = \frac{\sum_{h=1}^M \left[\mathbb{I}\{j \in u_{w_h}(t)\} \nabla_\theta \mathcal{L}_{w_h}(\theta_j^*(t)) \right]}{\sum_{h=1}^M \mathbb{I}\{j \in u_{w_h}(t)\}}.$$

We emphasize that here u_{w_h} and \mathcal{L}_{w_h} for all w_h can be computed very cheaply, enabling us to use a very large M to reduce the error of gradient estimation. Specifically, at iteration t , for each $j \in [m]$, we first calculate

$$\mathbf{L}(\theta_j^*(t)) = [\ell(x_1, f_{\theta_j^*(t)}), \dots, \ell(x_n, f_{\theta_j^*(t)})]^\top \in \mathbb{R}^n, \quad (10)$$

which is the vector encodes the loss of centroid j at each data point. This procedure does not introduce any extra computational overhead compared with standard gradient descent. After that, the bootstrap loss of centroid j can be computed cheaply by $\mathcal{L}_{\mathbf{w}}(\theta_j^*(t)) = \mathbf{w}^\top \mathbf{L}(\theta_j^*(t))$. Notice that as $\mathbf{L}(\theta_j^*(t))$ is pre-computed, calculating $\mathcal{L}_{\mathbf{w}}(\theta_j^*(t))$ for many (e.g., M) different \mathbf{w} is almost free, since it only requires a simple matrix multiplication with $O(nM)$ complexity. Similarly, it is cheap to obtain $u_{\mathbf{w}_h}$

$$u_{\mathbf{w}_h} = \arg \min_{j \in [m]} \mathbf{w}_h^\top \mathbf{L}(\theta_j^*(t)). \quad (11)$$

Taking the modified updating rule introduced to prevent the centroid degeneration phenomenon into account, we update $\theta_j^*(t)$ by $\theta_j^*(t+1) \leftarrow \theta_j^*(t) - \epsilon_t \phi(\theta_j^*(t))$, where

$$\phi(\theta_j^*) = \begin{cases} \hat{g}(\theta_j^*(t)) & \text{if } \sum_{h \in [M]} \mathbb{I}\{u_{\mathbf{w}_h}(t) = j\} / M > \gamma \\ \nabla_{\theta} \mathcal{L}(\theta_j^*(t)) & \text{otherwise.} \end{cases} \quad (12)$$

Note that as $u_{\mathbf{w}_h}(t)$ do not change much within a few iterations, in practice, we can update $u_{\mathbf{w}_h}(t)$ every a few iterations (e.g., every epoch). Specifically, at some iteration t , we sample \mathbf{w}_h i.i.d. from π and calculate $u_{\mathbf{w}_h}(t)$ for each h using (11). Then for the next a few iterations, we can reuse $u_{\mathbf{w}_h}(t)$ instead of re-calculating. Notice that in this case, we can also replace the $\nabla_{\theta} \mathcal{L}_{\mathbf{w}_h}(\theta_j^*(t))$ or $\nabla_{\theta} \mathcal{L}(\theta_j^*(t))$ in (12) using a mini-batch of data instead of the whole data, which leads to a stochastic gradient version of our algorithm. Algorithm 1 in Appendix B gives a summary.

4 Theory

Recall that, as discussed in (5), our approach relies on the intuition that bootstrap particles are nested in a small region so that we can approximate the distance between the centroid and a bootstrap particle by the bootstrap loss of that centroid. The main goal of this section is to give a formal theoretical justification of this intuition.

Before we proceed, we clarify several important setups for establishing and interpreting the theoretical result. As discussed in the introduction, we are mainly interested in the scenerio that the number of available particles/centroids m is small while the number of training data n is large, which motivates us to establish theoretical result in the region of small m and large n . This is significantly different from conventional asymptotic analysis in which we aim to show the behavior when $m \rightarrow \infty$.

We are mainly interested in characterizing the approximation of the proposed loss in (6) to the ideal loss in (3), given any small and fixed number m of centroids when $n \rightarrow \infty$. This justifies why the proposed centroid approximation method can be viewed as minimizing the Wasserstein distance between the particle distribution ρ_{π}^ and the target bootstrap distribution ρ_{π} .*

For simplicity, we build our analysis assuming the ideal update rule (8,9) is used. Analyzing how it changes when the practical update rule is conducted in an orthogonal direction and can be done using classic techniques in non-convex optimization. We start with the following main assumptions.

Assumption 1 (Smoothness and boundedness) Assume that the following quantities are upper bounded by some constant $c < \infty$:

$$\begin{aligned} & 1. \max_{i,j,k \in [d]} \sup_{\theta \in \Theta, x \in \mathcal{X}} \frac{\partial^3 \ell(x, f_\theta)}{\partial_i \theta_i \partial \theta_j \partial \theta_k}; & 2. \sup_{\theta_1, \theta_2 \in \Theta} \sup_{x \in \mathcal{X}} \frac{\|\nabla_\theta^2 \ell(x, f_{\theta_1}) - \nabla_\theta^2 \ell(x, f_{\theta_2})\|}{\|\theta_1 - \theta_2\|}; \\ & 3. \sup_{x \in \mathcal{X}, \theta \in \Theta} \|\nabla_\theta^2 \ell(x, f_\theta)\|; & 4. \sup_{\theta \in \Theta} \|\theta\|. \end{aligned}$$

Assumption 1 is a standard regularity condition on the boundness and smoothness of the problem.

Assumption 2 (Asymptotic normality) Assume $\sqrt{n}(\hat{\theta}_w - \theta) \xrightarrow{d} \mathcal{N}(0, A)$ and $\sqrt{n}(\hat{\theta} - \theta_0) \xrightarrow{d} \mathcal{N}(0, A)$ as $n \rightarrow \infty$, where A is a positive-definite matrix.

Assumption 2 is a higher level assumption on the asymptotic normality of the estimators. Such result is classic and can be derived with some weak and technical regularity conditions. See examples in Chatterjee et al. (2005); Cheng et al. (2010).

Assumption 3 (On the global minimizer) Suppose that $\lambda_{\min}(\nabla_\theta^2 \mathcal{L}_\infty(\theta_0)) > 0$.

Assumption 3 is also standard showing the locally strongly convexity of the loss around the truth θ_0 .

Assumption 4 (On the learning rate) Suppose that $\max_t \epsilon_t = O(n^{-1})$.

Assumption 4 assumes that the learning rate of the algorithm is sufficiently small such that its induced discretization error is not the dominating term.

The key challenge of our analysis is to show that our dynamics is $\mathcal{B}(\theta_0, r)$ -stable (defined below in Definition 1) for some small r , saying that $\{\theta_j^*(t)\}_{j=1}^m$ stay in a small region that is close to θ_0 for any iteration t . Combined with the property⁶ that $\hat{\theta}_w$ are also close to θ_0 , the centroids and the bootstrap particles are close to each other and thus our approximation in (5) holds for all $t \geq 0$. In this way, optimizing the centroids by minimizing our loss is almost equivalent to optimizing the centroids by minimizing the Wasserstein distance.

Definition 1 ($\mathcal{B}(\theta, r)$ -stable) Given some $\theta \in \Theta$ and $r \geq 0$, we say our dynamics is $\mathcal{B}(\theta, r)$ -stable if $\forall t \geq 0$ and $\forall j \in [m]$, $\theta_j^*(t) \in \mathcal{B}(\theta, r)$, where $\mathcal{B}(\theta, r) := \{\theta' : \|\theta' - \theta\| \leq r, \theta' \in \Theta\}$ is the ball with radius r centered at θ .

The key intuition to establish such $\mathcal{B}(\theta_0, r)$ -stable result is to characterize that our optimization dynamics is implicitly *self-controlled*: when some centroid approaches the boundary of $\mathcal{B}(\theta_0, r)$, the updating mechanism automatically start to push the centroid to move towards the center of the

⁶This is implied by the asymptotic normality in assumption 2.

			$m = 20$	$m = 50$	$m = 100$	$m = 200$
$\alpha = 0.9$	Normal	Bootstrap	0.029 ± 0.010	0.031 ± 0.011	0.021 ± 0.010	0.017 ± 0.010
		Centroid	0.027 ± 0.010	0.001 ± 0.009	0.012 ± 0.010	0.016 ± 0.010
	Percentile	Bootstrap	0.101 ± 0.013	0.036 ± 0.011	0.021 ± 0.010	0.014 ± 0.010
		Centroid	0.081 ± 0.012	0.021 ± 0.010	0.020 ± 0.010	0.015 ± 0.010
	Pivotal	Bootstrap	0.106 ± 0.013	0.045 ± 0.011	0.025 ± 0.010	0.023 ± 0.010
		Centroid	0.046 ± 0.011	0.013 ± 0.009	0.011 ± 0.010	0.020 ± 0.010

Table 1: Centroid approximation for confidence interval. The numbers in the table represent $|\alpha - \hat{\alpha}|$, where $\hat{\alpha}$ is the estimated coverage probability. The errors bar is the standard deviation.

region. Thus, if all the centroids are within $\mathcal{B}(\theta_0, r)$ at initialization, they will always stay in this region.

Thanks to assumption 2, 3, when the dataset is large, the landscape of our loss is locally strongly convex around θ_0 . When a centroid j is at the boundary of $\mathcal{B}(\theta_0, r)$, it has $v_j^*(t) < \gamma$ and thus the updating direction is the gradient of loss \mathcal{L} . By the convexity, such gradient will push the centroid move towards the center of $\mathcal{B}(\theta_0, r)$ where the empirical minimizer locates at. On the other hand, for centroid j with $v_j^*(t) \geq \gamma$, its updating direction aggregates information from sufficient data point and thus behaves similarly to that of the common gradient, pushing centroid to move towards the center with the centroid is not close to the center.

Theorem 1 *Under Assumptions 1-4 and suppose that we initialize $\theta_j^*(0)$, $j \in [m]$ by sampling from ρ_π , given any $m < \infty$ and $\gamma > 0$, we have*

$$\max_{j \in [m]} \sup_{t \geq 0} \|\theta_j^*(t) - \theta_0\| = O_p(\sqrt{(\log n)/n}).$$

Here the probability is taken w.r.t. training data.

Theorem 1 implies our dynamics is $\mathcal{B}(\theta_0, r_n)$ -stable with $r_n = O(\sqrt{\log n/n})$. The condition that $\theta_j^*(0) \sim \rho_\pi$ i.i.d. can be replaced by the condition that $\theta_j^*(0)$ is sufficiently close to θ_0 . We need such condition as we uniformly bound the distance between $\theta_j^*(t)$ and θ_0 at any iteration including the first one. Theorem 1 implies that the proposed loss in (6) is ‘almost as good as’ the ideal loss in (3).

Theorem 2 *Under the same assumptions as Theorem 1, given any $m < \infty$ and $\gamma > 0$, we have*

$$\sup_{t \geq 0} \left| \mathbb{E}_{\mathbf{w} \sim \pi} [\min_{j \in [m]} \mathcal{L}_{\mathbf{w}}(\theta_j^*(t))] - B - \mathbb{E}_{\mathbf{w} \sim \pi} [\min_{j \in [m]} \|\theta_j^*(t) - \hat{\theta}_{\mathbf{w}}\|_D^2] / 2 \right| = O_p(\sqrt{(\log n)/n^{3/2}}).$$

Here the probability is taken w.r.t. training data and B is some constant independent from $\theta_j^*(t)$ for any $t \geq 0$ and $j \in [m]$.

Asymptotics when m also grows Although our main interest is the asymptotics with a small, fixed m and growing n , we discuss here on asymptotics when m also grows. As shown in Section

3 and introduction, our method can be viewed as an ‘approximated’ K-means on the target distribution. From Theorem 5.2 in [Canas and Rosasco \(2012\)](#), the particle distribution formed by the optimal centroids learned by K-means gives improved $O(m^{-1/d})$ convergence to any general target distribution in terms of Wasserstein distance, where d is data dimension. In comparison, the particle distribution of i.i.d. sample only gives $O(m^{-1/(2d+4)})$ from Theorem 5.1 in [Canas and Rosasco \(2012\)](#). This implies that our approach potentially also has such a rate improvement. Note that the results in [Canas and Rosasco \(2012\)](#) are for general target distribution without any n involves. To rigorously establish the large m asymptotic result for our problem, we need to study the joint limit of n and m . This is indeed very non-trivial: as discussed in [Weed et al. \(2019\)](#) (i.e. Proposition 14), when $n \rightarrow \infty$, the target distribution ρ_π becomes a sharp Gaussian and the convergence rate of i.i.d. bootstrap particles will gradually improve to $O(m^{-1/2})$ (in a way that depends on n). It implies that when $n \gg m \rightarrow \infty$, our improvement may become only constant level. We find establishing such a theory is out the scope of this conference paper and leave it as future work.

5 Experiment

As discussed in the introduction, our main goal is to improve the quality of the particle distribution when only a limited number of particles/centroids is allowed, so that we can use less particles at deployment, which reduces the memory consumption and the computational cost for making prediction. Thus, our experiment design will be focusing on comparing the testing performance of vanilla bootstrap and our centroid based approach when the same and a small number of particles/centroids is used. We apply our method to four applications: confidence interval construction, bootstrap method in contextual bandit, bootstrapped deep Q-network and bagging. Due to space limit, we refer to Appendix C.4 for the bagging experiment, Appendix C.5 for ablation study on the importance of modifying the gradient to overcome the centroid degeneration phenomenon. Although we are less interested in the computational cost of training, as discussed in Section 3, our method actually only introduces a little training computation overhead, which is another advantage of our method. We draw analysis on this aspect in Appendix C.6.

5.1 Bootstrap Confidence Interval

We start with a classic application of bootstrap: confidence interval estimation for linear model with parameter θ . Fix confidence level α , we consider three ways to construct (two-sided) bootstrap confidence interval of θ : the Normal interval, the percentile interval and the pivotal interval. And we test $m = 20, 50, 100, 200$. For all experiments, we repeat with 1000 independent random trials. We consider the standard

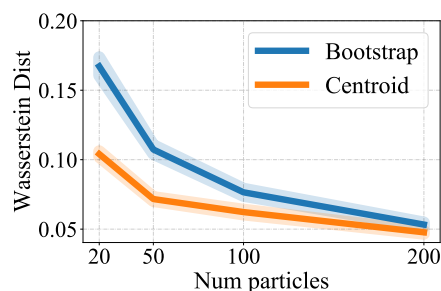


Figure 2: Wasserstein distance between the particle distribution and the true bootstrap distribution w.r.t. the number of particles.

		$m = 3$	$m = 4$	$m = 5$	$m = 10$
Mushroom	Bootstrap	3282.1 ± 72.82	3307.9 ± 69.2	3311.6 ± 79.3	3397.4 ± 51.4
	Centroid	3702.7 ± 89.76	3723.1 ± 78.7	3799.6 ± 84.2	3796.9 ± 36.1
Statlog	Bootstrap	1864.3 ± 6.4	1869.2 ± 5.2	1877.2 ± 4.1	1877.0 ± 2.7
	Centroid	1893.6 ± 6.0	1892.6 ± 3.6	1891.3 ± 3.5	1892.6 ± 2.8
Financial	Bootstrap	2255.77 ± 58.45	2265.42 ± 58.17	2269.33 ± 56.36	2281.35 ± 56.65
	Centroid	2313.29 ± 56.45	2315.32 ± 56.75	2323.88 ± 56.73	2325.54 ± 56.05

Table 2: Results on the contextual bandit experiment. The numbers in the table represent the averaged reward with its standard deviation.

bootstrap as baseline. Detailed experimental setup are included in Appendix C.1.

Figure 2 shows the Wasserstein distance between the true target distribution ρ_π and the empirical distributions obtained by (a) i.i.d. sampling $\hat{\rho}_\pi$, (b) the proposed centroid approximation ρ_π^* . The centroid approximation significantly reduces the Wasserstein distance by a large margin. We then compare the quality of obtained confidence intervals, which is measured by the difference between the estimated coverage probability and the true confidence level, i.e., $|\hat{\alpha} - \alpha|$ (the lower the better). Here we only consider confidence intervals of the first coordinate of θ : θ_1 . Table 1 summarizes the result with $\alpha = 0.9$. We see that using more particles is generally able to improve the constructed confidence intervals. We also compare with two variants of standard bootstrap: Bayesian bootstrap (Rubin, 1981) and residual bootstrap (Efron, 1992). And we consider varying $\alpha = 0.8, 0.95$. These results are included in Appendix C.1.

5.2 Centroid Approximation for Bootstrap Method in Contextual Bandit

Contextual bandit is a classic task in sequential decision making, in which accurately quantifying the model uncertainty is important in order to achieve good exploration-exploitation trade-off. As shown in Riquelme et al. (2018), tracking the model uncertainty using bootstrap is a strong method for contextual bandit. However, it is costly to maintain a large number of bootstrap models and thus the number of models is typically within 10 (Osband et al., 2016). We find that applying the proposed centroid approximation here can significantly improve the performance. Riquelme et al. (2018) uses $m = 3$ bootstrap models and we give a more comprehensive evaluation with $m = 3, 4, 5, 10$. We consider three datasets: Mushroom, Statlog and Financial. We set $\gamma = 0.5/m$. We randomly generate 20 different context sequences, apply all the methods and report the averaged cumulative reward and its standard deviation. Table 2 summarizes the result and note that a large part of variance can be explained by different context sequences. All results in Table 2 are statistically significant under significant level 5% using matched pair t-test. Table 2 shows that using more bootstrap models generally improves the accumulated reward. And when using the same number of models, the proposed centroid approximation method consistently improves over standard bootstrap method. We refer readers to appendix C.2 for more information on the background and experiment.

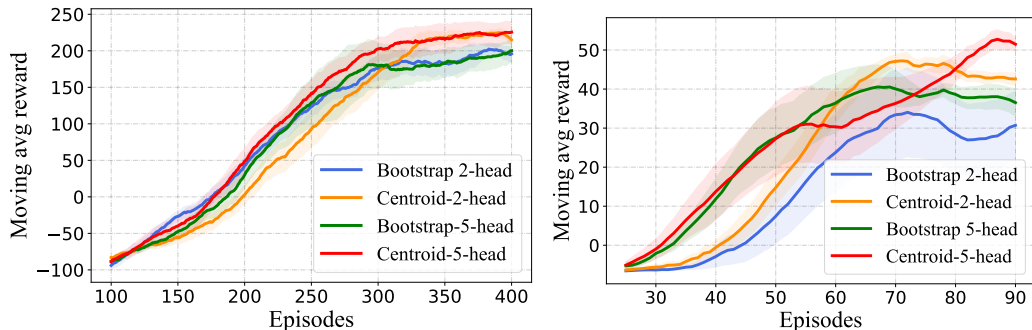


Figure 3: Results for Bootstrap DQN with centroid approximation experiment. Left: LunarLander-v2; Right: Catcher-v0.

5.3 Centroid Approximation for Bootstrap DQN

Efficient exploration is a major challenge for reinforcement learning (RL). Common dithering strategies such as ϵ -greedy do not carry out temporally-extended exploration, which leads to exponentially larger data requirements (Osband et al., 2016). To tackle this issue, Osband et al. (2016) proposes the Bootstrapped Deep Q-Network (DQN). We apply our centroid approximation to improve Bootstrapped DQN. We consider $m = 2, 5$ and similar to the experimental setting in contextual bandit, we set $\gamma = 0.5/m$. We consider two benchmark environments: LunarLander-v2 and Catcher-v0 from GYM (Brockman et al., 2016) and PyGame learning environment (Tasfi, 2016). We conduct the experiment with 5 independent random trails and report the averaged result with its standard deviation. We refer readers to Appendix C.3 for more background and other experiment details. Figure 3 summarizes the result. For LunarLander-v2, Bootstrap DQN with 2 and 5 heads give similar performance but both converge to a less optimal model compared with the centroid approximation method. Centroid approximation method with 2 and 5 heads performs similarly at convergence but centroid approximation method with 5 heads is able to converge faster than 2-head model and thus has lower regret. For Catcher-v0, adding more heads to the model is able to improve the performance for both methods. The proposed centroid approximation consistently improves over baselines.

6 Related Work

Bootstrap is an classical statistical inference method, which was developed by Efron (1992) and generalized by, i.e., Mammen (1993); Shao (2010); Efron (2012) (just to name a few). Bootstrap can be widely applied to various statistical inference problem, such as confidence interval estimation (DiCiccio et al., 1996), model selection (Shao, 1996), high-dimensional inference (Chen et al., 2018b; El Karoui and Purdom, 2018; Nie and Ročková, 2020), off-policy evaluation (Hanna et al., 2017), distributed inference (Yu et al., 2020) and inference for ensemble model (Kim et al., 2020), etc.

Despite its wide applications and nice theoretical properties, there has been very few works on discussing and improving the approximation efficiency *in the region of small bootstrap sample size*, beyond the i.i.d. sampling paradigm. While the m-out-of-n bootstrap (Bickel et al., 2012) and the bag of little bootstrap (Kleiner et al., 2014) are designed to reduce the computational cost with the subsampling techniques in the big data settings (large n), they still require a large bootstrap sample size and thus are still not scalable to large deep learning applications.

Bayesian Inference is a different approach to quantify the model uncertainty. Different from frequentists' method, Bayesian assumes a prior over the model and the uncertainty can be captured by the posterior. Bayesian inference have been largely popularized in machine learning, largely thanks to the recent development in scalable sampling method (Welling and Teh, 2011; Chen et al., 2014; Seita et al., 2016; Wu et al., 2020), variational inference (Blei et al., 2017; Liu and Wang, 2016), and other approximation methods such as Gal and Ghahramani (2016); Lee et al. (2018). In comparison, bootstrap has been much less widely used in modern machine learning and deep learning. We believe this is largely attributed to *the lack of similarly efficient computational methods in the small sample size m region*, which is the very problem that we aim to address with our new centroid approximation method. Note that there are also some optimization based approaches such as Chen et al. (2012, 2018a) that are able to improve the quality of the particles. However those approaches are not applicable to our setting as they need to access the ideal distribution.

Uncertainty in Deep Learning In additional to the applications considered in this paper, uncertainty in deep learning model can also be applied to problems including calibration (Guo et al., 2017) and out-of-distribution detection (Nguyen et al., 2015). The definition of uncertainty of neural network is quite generalized (e.g., Gal and Ghahramani (2016); Ovadia et al. (2019); Maddox et al. (2019); Van Amersfoort et al. (2020)) and can be quite different from the uncertainty that bootstrap inference want to quantify and can be approached with various methods including drop out (Gal and Ghahramani, 2016; Durasov et al., 2020), label smoothing (Qin et al., 2020), designing new modules in the model (Kivaranovic et al., 2020), adversarial training (Lakshminarayanan et al., 2016) and Bayesian modeling (Blundell et al., 2015), etc. This paper focuses on improving the bootstrap method and thus is orthogonal to those previous works. Pearce et al. (2018); Salem et al. (2020) also try to refine the ensemble models to improve the quality of prediction interval. Compare with our method, their method can only be applied to prediction interval and does not have theoretical guarantee.

7 Conclusion

We propose a centroid approximation method to learn an improved particle distribution that better approximates the target bootstrap distribution, especially in the region with small particle size. Theoretically, when the size of training data is large, our objective function is surrogate to the Wasserstein distance between the particle distribution and target distribution. Thus, compared with standard bootstrap, the proposed centroid approximation method actively optimizes the distance

between particle distribution and target distribution. The proposed method is simple and can be flexibly used for applications of bootstrap with negligible extra computational cost.

References

- Morgane Austern and Vasilis Syrgkanis. Asymptotics of the empirical bootstrap method beyond asymptotic normality. *arXiv preprint arXiv:2011.11248*, 2020.
- Peter J Bickel, Friedrich Götze, and Willem R van Zwet. Resampling fewer than n observations: gains, losses, and remedies for losses. In *Selected works of Willem van Zwet*, pages 267–297. Springer, 2012.
- David M Blei, Alp Kucukelbir, and Jon D McAuliffe. Variational inference: A review for statisticians. *Journal of the American statistical Association*, 112(518):859–877, 2017.
- Charles Blundell, Julien Cornebise, Koray Kavukcuoglu, and Daan Wierstra. Weight uncertainty in neural network. In *International Conference on Machine Learning*, pages 1613–1622. PMLR, 2015.
- Leo Breiman. Bagging predictors. *Machine learning*, 24(2):123–140, 1996.
- Greg Brockman, Vicki Cheung, Ludwig Pettersson, Jonas Schneider, John Schulman, Jie Tang, and Wojciech Zaremba. Openai gym. *arXiv preprint arXiv:1606.01540*, 2016.
- Guillermo Canas and Lorenzo Rosasco. Learning probability measures with respect to optimal transport metrics. In F. Pereira, C. J. C. Burges, L. Bottou, and K. Q. Weinberger, editors, *Advances in Neural Information Processing Systems*, volume 25. Curran Associates, Inc., 2012. URL <https://proceedings.neurips.cc/paper/2012/file/c54e7837e0cd0ced286cb5995327d1ab-Paper.pdf>.
- Snigdhanu Chatterjee, Arup Bose, et al. Generalized bootstrap for estimating equations. *The Annals of Statistics*, 33(1):414–436, 2005.
- Tianqi Chen, Emily Fox, and Carlos Guestrin. Stochastic gradient hamiltonian monte carlo. In *International conference on machine learning*, pages 1683–1691. PMLR, 2014.
- Wilson Ye Chen, Lester Mackey, Jackson Gorham, François-Xavier Briol, and Chris Oates. Stein points. In *International Conference on Machine Learning*, pages 844–853. PMLR, 2018a.
- Xiaohui Chen et al. Gaussian and bootstrap approximations for high-dimensional u -statistics and their applications. *The Annals of Statistics*, 46(2):642–678, 2018b.
- Yutian Chen, Max Welling, and Alex Smola. Super-samples from kernel herding. *arXiv preprint arXiv:1203.3472*, 2012.
- Guang Cheng, Jianhua Z Huang, et al. Bootstrap consistency for general semiparametric estimation. *Annals of Statistics*, 38(5):2884–2915, 2010.

- Thomas J DiCiccio, Bradley Efron, et al. Bootstrap confidence intervals. *Statistical science*, 11(3): 189–228, 1996.
- Nikita Durasov, Timur Bagautdinov, Pierre Baque, and Pascal Fua. Masksembles for uncertainty estimation. *arXiv preprint arXiv:2012.08334*, 2020.
- Bradley Efron. Bootstrap methods: another look at the jackknife. In *Breakthroughs in statistics*, pages 569–593. Springer, 1992.
- Bradley Efron. Bayesian inference and the parametric bootstrap. *The annals of applied statistics*, 6(4):1971, 2012.
- Noureddine El Karoui and Elizabeth Purdom. Can we trust the bootstrap in high-dimensions? the case of linear models. *The Journal of Machine Learning Research*, 19(1):170–235, 2018.
- Yarin Gal and Zoubin Ghahramani. Dropout as a bayesian approximation: Representing model uncertainty in deep learning. In *international conference on machine learning*, pages 1050–1059. PMLR, 2016.
- Alex Graves. Practical variational inference for neural networks. In *Advances in neural information processing systems*, pages 2348–2356. Citeseer, 2011.
- Chuan Guo, Geoff Pleiss, Yu Sun, and Kilian Q Weinberger. On calibration of modern neural networks. In *International Conference on Machine Learning*, pages 1321–1330. PMLR, 2017.
- Peter Hall et al. Rate of convergence in bootstrap approximations. *The Annals of Probability*, 16(4): 1665–1684, 1988.
- Josiah Hanna, Peter Stone, and Scott Niekum. Bootstrapping with models: Confidence intervals for off-policy evaluation. In *Proceedings of the AAAI Conference on Artificial Intelligence*, volume 31, 2017.
- Botao Hao, Yasin Abbasi-Yadkori, Zheng Wen, and Guang Cheng. Bootstrapping upper confidence bound. *arXiv preprint arXiv:1906.05247*, 2019.
- Jiri Hron, Alexander G de G Matthews, and Zoubin Ghahramani. Variational gaussian dropout is not bayesian. *arXiv preprint arXiv:1711.02989*, 2017.
- Gao Huang, Yixuan Li, Geoff Pleiss, Zhuang Liu, John E Hopcroft, and Kilian Q Weinberger. Snapshot ensembles: Train 1, get m for free. *arXiv preprint arXiv:1704.00109*, 2017.
- Byol Kim, Chen Xu, and Rina Foygel Barber. Predictive inference is free with the jackknife+-after-bootstrap. *arXiv preprint arXiv:2002.09025*, 2020.
- Danijel Kivaranovic, Kory D Johnson, and Hannes Leeb. Adaptive, distribution-free prediction intervals for deep networks. In *International Conference on Artificial Intelligence and Statistics*, pages 4346–4356. PMLR, 2020.

- Ariel Kleiner, Ameet Talwalkar, Purnamrita Sarkar, and Michael I Jordan. A scalable bootstrap for massive data. *Journal of the Royal Statistical Society: Series B: Statistical Methodology*, pages 795–816, 2014.
- Balaji Lakshminarayanan, Alexander Pritzel, and Charles Blundell. Simple and scalable predictive uncertainty estimation using deep ensembles. *arXiv preprint arXiv:1612.01474*, 2016.
- Jaehoon Lee, Jascha Sohl-dickstein, Jeffrey Pennington, Roman Novak, Sam Schoenholz, and Yasaman Bahri. Deep neural networks as gaussian processes. In *International Conference on Learning Representations*, 2018. URL <https://openreview.net/forum?id=B1EA-M-0Z>.
- Qiang Liu and Dilin Wang. Stein variational gradient descent: A general purpose bayesian inference algorithm. *arXiv preprint arXiv:1608.04471*, 2016.
- Wesley J Maddox, Pavel Izmailov, Timur Garipov, Dmitry P Vetrov, and Andrew Gordon Wilson. A simple baseline for bayesian uncertainty in deep learning. *Advances in Neural Information Processing Systems*, 32:13153–13164, 2019.
- Enno Mammen. Bootstrap and wild bootstrap for high dimensional linear models. *The annals of statistics*, pages 255–285, 1993.
- Benedict C May, Nathan Korda, Anthony Lee, and David S Leslie. Optimistic bayesian sampling in contextual-bandit problems. *Journal of Machine Learning Research*, 13:2069–2106, 2012.
- Anh Nguyen, Jason Yosinski, and Jeff Clune. Deep neural networks are easily fooled: High confidence predictions for unrecognizable images. In *Proceedings of the IEEE conference on computer vision and pattern recognition*, pages 427–436, 2015.
- Lizhen Nie and Veronika Ročková. Bayesian bootstrap spike-and-slab lasso. *arXiv preprint arXiv:2011.14279*, 2020.
- Ian Osband, Charles Blundell, Alexander Pritzel, and Benjamin Van Roy. Deep exploration via bootstrapped dqn. *arXiv preprint arXiv:1602.04621*, 2016.
- Yaniv Ovadia, Emily Fertig, Jie Ren, Zachary Nado, David Sculley, Sebastian Nowozin, Joshua V Dillon, Balaji Lakshminarayanan, and Jasper Snoek. Can you trust your model’s uncertainty? evaluating predictive uncertainty under dataset shift. *arXiv preprint arXiv:1906.02530*, 2019.
- Tim Pearce, Alexandra Brintrup, Mohamed Zaki, and Andy Neely. High-quality prediction intervals for deep learning: A distribution-free, ensembled approach. In *International Conference on Machine Learning*, pages 4075–4084. PMLR, 2018.
- Yao Qin, Xuezhi Wang, Alex Beutel, and Ed H Chi. Improving uncertainty estimates through the relationship with adversarial robustness. *arXiv preprint arXiv:2006.16375*, 2020.

- Carlos Riquelme, George Tucker, and Jasper Snoek. Deep bayesian bandits showdown: An empirical comparison of bayesian deep networks for thompson sampling. *arXiv preprint arXiv:1802.09127*, 2018.
- Donald B Rubin. The bayesian bootstrap. *The annals of statistics*, pages 130–134, 1981.
- Tárik S Salem, Helge Langseth, and Heri Ramampiaro. Prediction intervals: Split normal mixture from quality-driven deep ensembles. In *Conference on Uncertainty in Artificial Intelligence*, pages 1179–1187. PMLR, 2020.
- Daniel Seita, Xinlei Pan, Haoyu Chen, and John Canny. An efficient minibatch acceptance test for metropolis-hastings. *arXiv preprint arXiv:1610.06848*, 2016.
- Jun Shao. Bootstrap model selection. *Journal of the American statistical Association*, 91(434): 655–665, 1996.
- Xiaofeng Shao. The dependent wild bootstrap. *Journal of the American Statistical Association*, 105 (489):218–235, 2010.
- Karen Simonyan and Andrew Zisserman. Very deep convolutional networks for large-scale image recognition. *arXiv preprint arXiv:1409.1556*, 2014.
- Nitish Srivastava, Geoffrey Hinton, Alex Krizhevsky, Ilya Sutskever, and Ruslan Salakhutdinov. Dropout: a simple way to prevent neural networks from overfitting. *The journal of machine learning research*, 15(1):1929–1958, 2014.
- Norman Tasfi. Pygame learning environment. <https://github.com/ntasfi/PyGame-Learning-Environment>, 2016.
- William R Thompson. On the likelihood that one unknown probability exceeds another in view of the evidence of two samples. *Biometrika*, 25(3/4):285–294, 1933.
- Joost Van Amersfoort, Lewis Smith, Yee Whye Teh, and Yarin Gal. Uncertainty estimation using a single deep deterministic neural network. In *International Conference on Machine Learning*, pages 9690–9700. PMLR, 2020.
- Hado Van Hasselt, Arthur Guez, and David Silver. Deep reinforcement learning with double q-learning. In *Proceedings of the AAAI Conference on Artificial Intelligence*, volume 30, 2016.
- Apoorv Vyas, Nataraj Jammalamadaka, Xia Zhu, Dipankar Das, Bharat Kaul, and Theodore L Willke. Out-of-distribution detection using an ensemble of self supervised leave-out classifiers. In *Proceedings of the European Conference on Computer Vision (ECCV)*, pages 550–564, 2018.
- Larry Wasserman. *All of statistics: a concise course in statistical inference*. Springer Science & Business Media, 2013.
- Jonathan Weed, Francis Bach, et al. Sharp asymptotic and finite-sample rates of convergence of empirical measures in wasserstein distance. *Bernoulli*, 25(4A):2620–2648, 2019.

- Max Welling and Yee W Teh. Bayesian learning via stochastic gradient langevin dynamics. In *Proceedings of the 28th international conference on machine learning (ICML-11)*, pages 681–688. Citeseer, 2011.
- Tung-Yu Wu, YX Rachel Wang, and Wing H Wong. Mini-batch metropolis–hastings with reversible sgld proposal. *Journal of the American Statistical Association*, pages 1–9, 2020.
- Jeremy Wyatt. Exploration and inference in learning from reinforcement. 1998.
- Yang Yu, Shih-Kang Chao, and Guang Cheng. Simultaneous inference for massive data: Distributed bootstrap. In *International Conference on Machine Learning*, pages 10892–10901. PMLR, 2020.

A Proof

We also show Theorem 3, which gives a formal characterization of the Taylor approximation intuition introduced in (5).

Theorem 3 *Under Assumption 1 and 2, when n is sufficiently large, we have*

$$\begin{aligned} \mathcal{L}_{\mathbf{w}}(\theta) &= \mathcal{L}_{\mathbf{w}}(\hat{\theta}_{\mathbf{w}}) + \frac{1}{2} \left(\theta - \hat{\theta}_{\mathbf{w}} \right)^\top \nabla_{\theta}^2 \mathcal{L}_{\infty}(\theta_0) \left(\theta - \hat{\theta}_{\mathbf{w}} \right) \\ &\quad + O_p \left(\|\theta - \hat{\theta}_{\mathbf{w}}\|^2 (n^{-1/2} + \|\theta - \hat{\theta}_{\mathbf{w}}\|) \right). \end{aligned}$$

Here the stochastic boundedness is taken w.r.t. the training data and \mathbf{w} .

In the proof, we may use c to represent some absolute constant, which may vary in different lines.

A.1 Proof of Theorem 3

With the fact that $\nabla_{\mathbf{w}} \mathcal{L}(\hat{\theta}_{\mathbf{w}}) = 0$ and under assumption 1, using Taylor expansion, we have

$$\mathcal{L}_{\mathbf{w}}(\theta) = \mathcal{L}_{\mathbf{w}}(\hat{\theta}_{\mathbf{w}}) + \frac{1}{2} \left(\theta - \hat{\theta}_{\mathbf{w}} \right)^\top \nabla_{\theta}^2 \mathcal{L}_{\mathbf{w}}(\hat{\theta}_{\mathbf{w}}) \left(\theta - \hat{\theta}_{\mathbf{w}} \right) + O \left(\|\theta - \hat{\theta}_{\mathbf{w}}\|^3 \right).$$

Notice that

$$\begin{aligned} &\left| \left(\theta - \hat{\theta}_{\mathbf{w}} \right)^\top \left(\nabla_{\theta}^2 \mathcal{L}_{\mathbf{w}}(\hat{\theta}_{\mathbf{w}}) - \nabla_{\theta}^2 \mathcal{L}_{\infty}(\theta_0) \right) \left(\theta - \hat{\theta}_{\mathbf{w}} \right) \right| \\ &\leq \|\theta - \hat{\theta}_{\mathbf{w}}\|^2 \left\| \nabla_{\theta}^2 \mathcal{L}_{\mathbf{w}}(\hat{\theta}_{\mathbf{w}}) - \nabla_{\theta}^2 \mathcal{L}_{\infty}(\theta_0) \right\| \\ &\leq \|\theta - \hat{\theta}_{\mathbf{w}}\|^2 \left(\left\| \nabla_{\theta}^2 \mathcal{L}_{\mathbf{w}}(\hat{\theta}_{\mathbf{w}}) - \nabla_{\theta}^2 \mathcal{L}_{\mathbf{w}}(\theta_0) \right\| + \left\| \nabla_{\theta}^2 \mathcal{L}_{\mathbf{w}}(\theta_0) - \nabla_{\theta}^2 \mathcal{L}_{\infty}(\theta_0) \right\| \right) \\ &\leq \|\theta - \hat{\theta}_{\mathbf{w}}\|^2 \left(C \|\hat{\theta}_{\mathbf{w}} - \theta_0\| + \left\| \nabla_{\theta}^2 \mathcal{L}_{\mathbf{w}}(\theta_0) - \nabla_{\theta}^2 \mathcal{L}_{\infty}(\theta_0) \right\|_F \right), \end{aligned}$$

where we denote the Frobenius norm as $\|\cdot\|_F$. With assumption 2, we have $\|\hat{\theta}_{\mathbf{w}} - \theta_0\| = O_p(n^{-1/2})$.

By applying centroid limit theorem and delta method to $\left| \nabla_{\theta_{ij}}^2 \mathcal{L}_{\mathbf{w}}(\theta_0) - \nabla_{\theta_{ij}}^2 \mathcal{L}_{\infty}(\theta_0) \right|$ for every pair $i, j \in [d]$, we have $\left\| \nabla_{\theta}^2 \mathcal{L}_{\mathbf{w}}(\theta_0) - \nabla_{\theta}^2 \mathcal{L}_{\infty}(\theta_0) \right\|_F = O_p(n^{-1/2})$. Thus we obtained the desired result.

A.2 Proof of Theorem 1

Given any radius r , with sufficiently large n , we have

$$\mathbb{P} \left(\|\hat{\theta}_{\mathbf{w}} - \theta_0\| \geq r \right) \leq \exp(-\lambda n r^2),$$

for $\lambda = \frac{1}{4}\lambda_{\min}(A)$. Here the probability is the jointly probability of bootstrap weight and training data. Thus, given any r , under the assumption that $\theta_j^*(0)$ is initialized via sampling $\hat{\theta}_w$, then we have

$$\mathbb{P}(\cup_{j \in [m]} \{\|\theta_j^*(0) - \theta_0\| \geq r\}) \leq \sum_{j \in [m]} \mathbb{P}(\|\theta_j^*(0) - \theta_0\| \geq r) \leq m \exp(-\lambda nr^2).$$

We proof by induction. Given any $\{\theta_j\}_{j=1}^m$, define

$$R_{k,r} = \mathbb{I} \left\{ w \in \text{supp}(\pi) : \arg \min_{j \in [m]} \mathcal{L}_w(\theta_j) = k \text{ and } \|\hat{\theta}_w - \theta_0\| \leq r \right\}.$$

Suppose at iteration t , we have $\|\theta_k^*(t) - \theta_0\| \leq \frac{c\alpha\sqrt{\frac{\log n}{n}}}{\lambda_0\gamma}$ for some constant c and λ_0 , which we denote as the minimum eigenvalue of $\nabla_{\theta}^2 \mathcal{L}_{\infty}(f_{\theta_0})$. Now at iteration t , we have two cases.

Case 1: $\mathbb{E}_{\pi} R_{k,\infty} \geq \gamma$ Suppose that at iteration t , for k such that $\mathbb{E}_{\pi} R_{k,\infty} \geq \gamma$, and $\|\theta_k^*(t) - \theta_0\| = q_k$, we have the following property:

$$\begin{aligned} \|\theta_k^*(t+1) - \theta_0\|^2 &= \left\| \theta_k^*(t) - \frac{\epsilon_t}{\mathbb{E}_{\pi} R_{k,\infty}} \mathbb{E}_{\pi} [\nabla_{\theta} \mathcal{L}_w(\theta_k^*(t)) R_{k,\infty}] - \theta_0 \right\|^2 \\ &= \|\theta_k^*(t) - \theta_0\|^2 - \frac{2\epsilon_t}{\mathbb{E}_{\pi} R_{k,\infty}} \langle \theta_k^*(t) - \theta_0, \mathbb{E}_{\pi} [\nabla_{\theta} \mathcal{L}_w(\theta_k^*(t)) R_{k,\infty}] \rangle \\ &\quad + \epsilon_t^2 \|\mathbb{E}_{\pi} [\nabla_{\theta} \mathcal{L}_w(\theta_k^*(t)) R_{k,\infty}]\|^2. \end{aligned}$$

Notice that

$$\begin{aligned} \mathbb{E}_{\pi} [\nabla_{\theta} \mathcal{L}_w(\theta_k^*(t)) R_{k,q_k}] &\stackrel{(1)}{=} \mathbb{E}_{\pi} \left[\nabla_{\theta}^2 \mathcal{L}_w(\hat{\theta}_w)(\theta_k^*(t) - \hat{\theta}_w) R_{k,q_k} \right] + o(q_k^2) \\ &\stackrel{(2)}{=} \mathbb{E}_{\pi} \left[\nabla_{\theta}^2 \mathcal{L}_w(\hat{\theta}_w)(\theta_k^*(t) - \theta_0) R_{k,q_k} \right] + O(q_k^2) \\ &\stackrel{(3)}{=} \mathbb{E}_{\pi} \left[\nabla_{\theta}^2 \mathcal{L}_w(\theta_0)(\theta_k^*(t) - \theta_0) R_{k,q_k} \right] + O(q_k^2) \end{aligned}$$

Here (1) is obtained via applying Taylor expansion on $\nabla_{\theta} \mathcal{L}_w(\theta_k^*(t))$ at $\hat{\theta}_w$. (2) is by assumption 1 and 2. (3) is by assumption 1. We thus have

$$\begin{aligned} & - \langle \theta_k^*(t) - \theta_0, \mathbb{E}_{\pi} [\nabla_{\theta} \mathcal{L}_w(\theta_k^*(t)) R_{k,\infty}] \rangle \\ & \leq - \langle \theta_k^*(t) - \theta_0, \mathbb{E}_{\pi} [\nabla_{\theta} \mathcal{L}_w(\theta_k^*(t)) R_{k,q_k}] \rangle + \|\theta_k^*(t) - \theta_0\| \|\mathbb{E}_{\pi} \nabla_{\theta} \mathcal{L}_w(\theta_k^*(t))(1 - R_{k,q_k})\| \\ & \leq - \langle \theta_k^*(t) - \theta_0, \mathbb{E}_{\pi} [\nabla_{\theta} \mathcal{L}_w(\theta_k^*(t)) R_{k,q_k}] \rangle + cq_k \exp(-\lambda nq_k^2) \\ & \leq - \mathbb{E}_{\pi} R_{k,q_k} (\theta_k^*(t) - \theta_0)^{\top} \nabla_{\theta}^2 \mathcal{L}_w(\theta_0) (\theta_k^*(t) - \theta_0) + cq_k \exp(-\lambda nq_k^2) + O(q_k^3). \end{aligned}$$

Notice that with sufficiently large n , with central limit theorem, we have

$$\begin{aligned}
& -\mathbb{E}_\pi R_{k,q_k}(\theta_k^*(t) - \theta_0)^\top \nabla_\theta^2 \mathcal{L}_w(\theta_0)(\theta_k^*(t) - \theta_0) \\
& \leq \|\theta_k^*(t) - \theta_0\|^2 \mathbb{E}_\pi \left\| \nabla_\theta^2 \mathcal{L}_w(\theta_0) - \nabla_\theta^2 \mathcal{L}_w(\theta_0) \right\| - \mathbb{E}_\pi R_{k,q_k}(\theta_k^*(t) - \theta_0)^\top \nabla_\theta^2 \mathcal{L}_\infty(\theta_0)(\theta_k^*(t) - \theta_0) \\
& = -\mathbb{E}_\pi R_{k,q_k}(\theta_k^*(t) - \theta_0)^\top \nabla_\theta^2 \mathcal{L}_\infty(\theta_0)(\theta_k^*(t) - \theta_0) + O(n^{-1/2}).
\end{aligned}$$

This gives that

$$\begin{aligned}
& -\langle \theta_k^*(t) - \theta_0, \mathbb{E}_\pi [\nabla_\theta \mathcal{L}_w(\theta_k^*(t)) R_{k,\infty}] \rangle \\
& \leq -\mathbb{E}_\pi R_{k,q_k}(\theta_k^*(t) - \theta_0)^\top \nabla_\theta^2 \mathcal{L}_\infty(\theta_0)(\theta_k^*(t) - \theta_0) + cq_k \exp(-\lambda n q_k^2) + O\left(q_k^3 + q_k n^{-1/2}\right) \\
& \leq -\lambda_0 \mathbb{E}_\pi R_{k,q_k} \|\theta_k^*(t) - \theta_0\|^2 + cq_k \exp(-\lambda n q_k^2) + O\left(q_k^3 + q_k n^{-1/2}\right).
\end{aligned}$$

Use the above estimation, we have

$$\begin{aligned}
& \|\theta_k^*(t+1) - \theta_0\|^2 \\
& \leq \|\theta_k^*(t) - \theta_0\|^2 - 2\epsilon_t \lambda_{\min} \frac{\mathbb{E}_\pi R_{k,q_k}}{\mathbb{E}_\pi R_{k,\infty}} \|\theta_k^*(t) - \theta_0\|^2 \\
& + 2c\epsilon_t q_k \exp(-\lambda n q_k^2) / \mathbb{E}_\pi R_{k,\infty} + O\left(\epsilon_t (q_k^3 + q_k n^{-1/2}) / \mathbb{E}_\pi R_{k,\infty} + \epsilon_t^2\right) \\
& \leq \|\theta_k^*(t) - \theta_0\|^2 + \frac{\epsilon_t}{\mathbb{E}_\pi R_{k,\infty}} \left(-2\lambda_0 \mathbb{E}_\pi R_{k,q_k} \|\theta_k^*(t) - \theta_0\|^2 - 2cq_k \exp(-\lambda n q_k^2) + O\left(q_k^3 + \epsilon_t + q_k n^{-1/2}\right)\right).
\end{aligned}$$

Notice that by choosing $\alpha > \sqrt{1/(2\lambda)}$ and $\epsilon_t = O(n^{-1})$, with sufficiently large n , when

$$\|\theta_k^*(t) - \theta_0\| \geq \frac{c\alpha \sqrt{\frac{\log n}{n}}}{\lambda_0 \mathbb{E}_\pi R_{k,q_k}}$$

for some constant c , we have

$$\|\theta_k^*(t+1) - \theta_0\| \leq \|\theta_k^*(t) - \theta_0\|.$$

Thus $\|\theta_k^*(t+1) - \theta_0\| \leq \frac{c\alpha \sqrt{\frac{\log n}{n}}}{\lambda_0 \mathbb{E}_\pi R_{k,\infty}} \leq \frac{c\alpha \sqrt{\frac{\log n}{n}}}{\lambda_0 \gamma}$ for some constant c .

Case 2: $\mathbb{E}_\pi R_{k,\infty} \leq \gamma$ In this case, we have

$$\begin{aligned}
\|\theta_k^*(t+1) - \theta_0\|^2 & = \left\| \theta_k^*(t) - \epsilon_t \nabla_\theta \mathcal{L}(f_{\theta_k^*(t)}) - \theta_0 \right\|^2 \\
& = \|\theta_k^*(t) - \theta_0\|^2 - 2\epsilon_t \langle \theta_k^*(t) - \theta_0, \nabla_\theta \mathcal{L}(\theta_k^*(t)) \rangle + \epsilon_t^2 \left\| \nabla_\theta \mathcal{L}(f_{\theta_k^*(t)}) \right\|^2.
\end{aligned}$$

Notice that

$$\begin{aligned}
& - \langle \theta_k^*(t) - \theta_0, \nabla_{\theta} \mathcal{L}(\theta_k^*(t)) \rangle \\
& \leq - \langle \theta_k^*(t) - \theta_0, \nabla_{\theta}^2 \mathcal{L}(\theta_0) (\theta_k^*(t) - \theta_0) \rangle - \langle \theta_k^*(t) - \theta_0, \nabla_{\theta} \mathcal{L}(f_{\theta_0}) \rangle + o(\|\theta_k^*(t) - \theta_0\|^3) \\
& = - (\theta_k^*(t) - \theta_0)^{\top} \nabla_{\theta}^2 \mathcal{L}_{\infty}(\theta_0) (\theta_k^*(t) - \theta_0) + o(\|\theta_k^*(t) - \theta_0\|^3) + O_p(n^{-1/2}) \|\theta_k^*(t) - \theta_0\|.
\end{aligned}$$

This gives that

$$\|\theta_k^*(t+1) - \theta_0\|^2 \leq \|\theta_k^*(t) - \theta_0\|^2 - 2\epsilon_t \lambda_0 \|\theta_k^*(t) - \theta_0\|^2 + o(\epsilon_t \|\theta_k^*(t) - \theta_0\|^3 + \epsilon_t^2) + O_p(n^{-1/2}) \epsilon_t \|\theta_k^*(t) - \theta_0\|.$$

With $\epsilon_t = O(n^{-1})$ and sufficiently large n , when

$$\|\theta_k^*(t) - \theta_0\| \geq \frac{c\alpha \sqrt{\frac{\log n}{n}}}{\lambda_0 \gamma},$$

we have $\|\theta_k^*(t+1) - \theta_0\|^2 \leq \|\theta_k^*(t) - \theta_0\|^2$.

Combine this two cases, we conclude that $\|\theta_k^*(t+1) - \theta_0\| \leq \frac{c\alpha \sqrt{\frac{\log n}{n}}}{\lambda_0 \gamma}$ for any t , when $\|\theta_k^*(0) - \theta_0\| \leq \frac{c\alpha \sqrt{\frac{\log n}{n}}}{\lambda_0 \gamma}$. We thus conclude that, for any $\alpha > \sqrt{1/(2\lambda)}$, with probability at least $1 - m \exp\left(-\lambda \frac{c\alpha^2 \log n}{\lambda_0^2 \gamma^2}\right)$, we have

$$\max_{j \in [m]} \sup_t \|\theta_j^*(t) - \theta_0\| \leq \frac{c\alpha \sqrt{\frac{\log n}{n}}}{\lambda_0 \gamma}.$$

A.3 Proof for Theorem 2

Notice that

$$\begin{aligned}
& \mathcal{L}_{\mathbf{w}}(\theta_j^*(t)) - \mathcal{L}_{\mathbf{w}}(\hat{\theta}_{\mathbf{w}}) \\
& = \frac{1}{2} (\theta_j^*(t) - \hat{\theta}_{\mathbf{w}})^{\top} \nabla_{\theta}^2 \mathcal{L}_{\mathbf{w}}(\hat{\theta}_{\mathbf{w}}) (\theta_j^*(t) - \hat{\theta}_{\mathbf{w}}) + O(\|\theta_j^*(t) - \hat{\theta}_{\mathbf{w}}\|^3) \\
& = \frac{1}{2} (\theta_j^*(t) - \hat{\theta}_{\mathbf{w}})^{\top} \nabla_{\theta}^2 \mathcal{L}_{\mathbf{w}}(\theta_0) (\theta_j^*(t) - \hat{\theta}_{\mathbf{w}}) + O(\|\theta_j^*(t) - \hat{\theta}_{\mathbf{w}}\|^3) + O(\|\theta_j^*(t) - \hat{\theta}_{\mathbf{w}}\|^2 \|\hat{\theta}_{\mathbf{w}} - \theta_0\|) \\
& = \frac{1}{2} \|\theta_j^*(t) - \hat{\theta}_{\mathbf{w}}\|_D^2 + \|\nabla_{\theta}^2 \mathcal{L}_{\mathbf{w}}(\theta_0) - \nabla_{\theta}^2 \mathcal{L}_{\infty}(\theta_0)\| \|\theta_j^*(t) - \hat{\theta}_{\mathbf{w}}\|^2 + O(\|\theta_j^*(t) - \hat{\theta}_{\mathbf{w}}\|^3) \\
& + O(\|\theta_j^*(t) - \hat{\theta}_{\mathbf{w}}\|^2 \|\hat{\theta}_{\mathbf{w}} - \theta_0\|)
\end{aligned}$$

Given \mathbf{w} , we define $u_{\mathbf{w}} = \arg \min_{j \in [m]} \|\theta_j^*(t) - \hat{\theta}_{\mathbf{w}}\|_D^2$. For any $\alpha > \sqrt{1/(2\lambda)}$, with probability

Algorithm 1 Algorithm for Centroid Approximation

- 1: Initialize $\theta_j^*(0), j \in [m]$ by i.i.d. sampling from ρ_π or other distribution such as Gaussian.
 - 2: **for** $t \in$ outer-iters **do**
 - 3: Calculate $\mathbf{L}(\theta_j^*(t)), \forall j \in [m]$;
 - 4: Sample $\mathbf{w}_h, h \in [M]$ i.i.d. from π and calculate $u_{\mathbf{w}_h}(t)$ by (11) for each h .
 - 5: **for** $t' \in$ inner-iters **do**
 - 6: **for** $j \in [m]$ **do**
 - 7: Update the j -th centroid via (12) (May use mini-batch gradient).
 - 8: **end for**
 - 9: **end for**
 - 10: **end for**
-

at least $1 - m \exp\left(-\lambda \frac{c\alpha^2 \log n}{\lambda_0^2 \gamma^2}\right)$, we have

$$\begin{aligned} & \frac{1}{2} \mathbb{E}_{\mathbf{w} \sim \pi} \left[\min_{j \in [m]} \|\theta_j^*(t) - \hat{\theta}_{\mathbf{w}}\|_D^2 \right] \\ &= \frac{1}{2} \mathbb{E}_{\mathbf{w} \sim \pi} \left[\|\theta_{u_{\mathbf{w}}}^* - \hat{\theta}_{\mathbf{w}}\|_D^2 \right] \\ &\geq \mathbb{E}_{\mathbf{w} \sim \pi} \left[\mathcal{L}_{\mathbf{w}}(\theta_{u_{\mathbf{w}}}^*) - \mathcal{L}_{\mathbf{w}}(\hat{\theta}_{\mathbf{w}}) - c \|\theta_{u_{\mathbf{w}}}^* - \hat{\theta}_{\mathbf{w}}\|^2 \left(\|\hat{\theta}_{\mathbf{w}} - \theta_0\| + \|\nabla_{\hat{\theta}}^2 \mathcal{L}_{\mathbf{w}}(\theta_0) - \nabla_{\hat{\theta}}^2 \mathcal{L}_{\infty}(\theta_0)\| + \|\theta_{u_{\mathbf{w}}}^* - \hat{\theta}_{\mathbf{w}}\| \right) \right] \\ &\geq \mathbb{E}_{\mathbf{w} \sim \pi} \left[\mathcal{L}_{\mathbf{w}}(\theta_{u_{\mathbf{w}}}^*) \right] - \mathbb{E}_{\mathbf{w} \sim \pi} \left[\mathcal{L}_{\mathbf{w}}(\hat{\theta}_{\mathbf{w}}) \right] - c \left(\frac{\alpha \sqrt{\log n}}{\lambda_0 \gamma n^{3/2}} \right) \\ &= \mathbb{E}_{\mathbf{w} \sim \pi} \left[\min_{j \in [m]} \mathcal{L}_{\mathbf{w}}(\theta_j^*(t)) \right] - \mathbb{E}_{\mathbf{w} \sim \pi} \left[\mathcal{L}_{\mathbf{w}}(\hat{\theta}_{\mathbf{w}}) \right] - c \left(\frac{\alpha \sqrt{\log n}}{\lambda_0 \gamma n^{3/2}} \right). \end{aligned}$$

Similarly, we also have, with probability at least $1 - m \exp\left(-\lambda \frac{c\alpha^2 \log n}{\lambda_0^2 \gamma^2}\right)$,

$$\mathbb{E}_{\mathbf{w} \sim \pi} \left[\min_{j \in [m]} \mathcal{L}_{\mathbf{w}}(\theta_j^*(t)) \right] - \mathbb{E}_{\mathbf{w} \sim \pi} \left[\mathcal{L}_{\mathbf{w}}(\hat{\theta}_{\mathbf{w}}) \right] \geq \frac{1}{2} \mathbb{E}_{\mathbf{w} \sim \pi} \left[\min_{j \in [m]} \|\theta_j^*(t) - \hat{\theta}_{\mathbf{w}}\|_D^2 \right] - c \left(\frac{\alpha \sqrt{\log n}}{\lambda_0 \gamma n^{3/2}} \right).$$

Notice that the above bound holds uniformly for all $j \in [m]$ and any iteration t , which implies that with probability at least $1 - 2m \exp\left(-\lambda \frac{c\alpha^2 \log n}{\lambda_0^2 \gamma^2}\right)$, we have

$$\sup_{t \geq 0} \left| \mathbb{E}_{\mathbf{w} \sim \pi} \left[\min_{j \in [m]} \mathcal{L}_{\mathbf{w}}(\theta_j^*(t)) \right] - B - \mathbb{E}_{\mathbf{w} \sim \pi} \left[\min_{j \in [m]} \|\theta_j^*(t) - \hat{\theta}_{\mathbf{w}}\|_D^2 / 2 \right] \right| \leq c \left(\frac{\alpha \sqrt{\log n}}{\lambda_0 \gamma n^{3/2}} \right).$$

B Algorithm Box

We provide the algorithm box in Algorithm 1 for practical implementations.

C Additional Experiment details

C.1 Bootstrap Confidence Interval

Given a model f_θ parameterized by θ and a training set with n data points i.i.d. sampled from population, our goal is to construct confidence interval for θ . Let $\tilde{\rho}_\pi$ be an empirical distribution approximating ρ_π , which could be obtained by i.i.d. sampling, or by our centroid method. Denote by $Q[\alpha, \tilde{\rho}_\pi]$ the α -quantile function of $\tilde{\rho}_\pi$ with some $\alpha \in [0, 1]$. We consider the following three ways to construct (two-sided) bootstrap confidence interval of θ with confidence level α : the Normal interval, the percentile interval and the pivotal interval which are defined below.

Methods to construct confidence interval The methods we used to construct confidence interval are – The Normal interval:

$$[\hat{\theta} - z((1 + \alpha)/2)\hat{s}_{\text{boot}}, \hat{\theta} + z((1 + \alpha)/2)\hat{s}_{\text{boot}}],$$

where $z(\cdot)$ is the inverse cumulative distribution function of standard Normal distribution. And \hat{s}_{boot} is the standard deviation estimated from $\tilde{\rho}_\pi$.

– The percentile intervals:

$$[Q[(1 - \alpha)/2, \hat{\rho}_\pi], Q[(1 + \alpha)/2, \hat{\rho}_\pi]].$$

– The pivotal interval:

$$[2\hat{\theta} - Q[(1 + \alpha)/2, \hat{\rho}_\pi], 2\hat{\theta} - Q[(1 - \alpha)/2, \hat{\rho}_\pi]].$$

We consider the following simple linear regression: $x \sim \mathcal{N}(\mathbf{0}, \mathbf{I})$, $y | x \sim \mathcal{N}(\theta^\top x, \mathbf{I})$, where the features $x \in \mathbb{R}^4$ and we set the true parameter to be $\theta_0 = [1, -1, 1, -1]$. We consider $n = 50$ and the number of particles $m = 20, 50, 100, 200$. We compare the coverage probability and the confidence level α to measure the quality:

Measuring the quality of confidence interval With a large number N of independently generated training data (we use $N = 1000$), we are able to obtain the corresponding confidence intervals $\{\text{CI}(\alpha)_s\}_{s=1}^N$ and thus obtain the probability that the true parameter falls into the confidence intervals, which is the estimated coverage probability

$$\hat{\alpha} = \frac{1}{N} \sum_{s=1}^N \mathbb{I}\{\theta_0 \in \text{CI}(\alpha)_s\}.$$

A good confidence interval should have $\hat{\alpha}$ close to α . Thus we measure the performance by calculating the difference $|\alpha - \hat{\alpha}|$.

As $\hat{\theta}_w$ is the least square estimator of the bootstrapped dataset, it has analytic solution and thus can be obtained via some matrix multiplications. θ_w^* is initialized using $\hat{\theta}_w$ and then updated for 2000 steps. For this experiment, we find that adding the threshold γ does not give further improvement for this experiment and thus we simply set $\gamma = 0$ and use $M = 1$. We approximate the true bootstrap distribution by sampling 10000 i.i.d. samples.

More experiment result Table 3 all the result we have varying $\alpha = 0.8, 0.9, 0.95$, $m = 20, 50, 100, 200$ and three different approaches for constructing confidence interval. As we can see, centroid approximation gives the best performance in most cases compared with the other three baselines.

C.2 Centroid Approximation for Bootstrap Method in Contextual Bandit

More background Contextual bandit is a classic task in sequential decision making problem in which at time $t = 1, \dots, n$, a new context x_t arrives and is observed by an algorithm. Based on its internal model, the algorithm selects an actions a_t and receives a reward $r_t(x_t, a_t)$ related to the context and action. During this process, the algorithm may update its internal model with the newly received data. At the end of this process, the cumulative reward of the algorithm is calculated by $r = \sum_{t=1}^n r_t$ and the goal for the algorithm is to improve the cumulative reward r . The exploration-exploitation dilemma is a fundamental aspect in sequential decision making problem such as contextual bandit: the algorithm needs to trade-off between the best expected action returned by the internal model at the moment (i.e., exploitation) with potentially sub-optimal exploratory actions. Thompson sampling (Thompson, 1933; Wyatt, 1998; May et al., 2012) is an elegant and effective approach to tackle the exploration-exploitation dilemma using the model uncertainty, which can be approached with various methods including Bayesian posterior (Graves, 2011; Welling and Teh, 2011), dropout uncertainty (Srivastava et al., 2014; Hron et al., 2017) and Bootstrap (Osband et al., 2016; Hao et al., 2019). The ability to accurately assess the uncertainty is a key to improve the cumulative reward. Bootstrap method for contextual bandit maintains m bootstrap models trained with different bootstrapped training set. When conducting an action, the algorithm uniformly samples a model and then selects the best action returned by the sampled model.

More experiment setup details We set all the experimental setting including data preprocessing, network architecture and training pipeline exactly the same as the one used in Riquelme et al. (2018) and adopt its open source code repository. Specifically, we consider a fully connected feed forward network with two hidden layers with 50 hidden units and ReLU activations. The input and output dimensions depends on the dimension of context and number of possible actions. For each data set, we randomly generate 2000 contexts and we for each algorithm, we update the replay memory buffer for each model as well as train each model every 50 contexts. During each model updating, each model is trained for 100 iterations with batch size 512. Riquelme et al. (2018) consider update the replay buffer for each model by resampling the latest 50 contexts and their outcomes without

Num Particle		20	50	100	200	
$\alpha = 0.8$	Normal	Bootstrap	0.033 ± 0.013	0.028 ± 0.013	0.026 ± 0.013	0.031 ± 0.013
		Bayesian	0.084 ± 0.014	0.076 ± 0.014	0.082 ± 0.014	0.086 ± 0.014
		Residual	0.033 ± 0.013	0.037 ± 0.013	0.029 ± 0.013	0.024 ± 0.013
		Centroid	0.036 ± 0.013	0.003 ± 0.012	0.017 ± 0.013	0.030 ± 0.013
	Percentile	Bootstrap	0.096 ± 0.014	0.050 ± 0.014	0.044 ± 0.013	0.024 ± 0.013
		Bayesian	0.114 ± 0.015	0.079 ± 0.014	0.074 ± 0.014	0.071 ± 0.014
		Residual	0.079 ± 0.014	0.032 ± 0.013	0.017 ± 0.013	0.010 ± 0.013
		Centroid	0.066 ± 0.014	0.008 ± 0.013	0.019 ± 0.013	0.020 ± 0.013
	Pivotal	Bootstrap	0.101 ± 0.015	0.053 ± 0.014	0.045 ± 0.014	0.033 ± 0.013
		Bayesian	0.158 ± 0.015	0.110 ± 0.110	0.088 ± 0.014	0.078 ± 0.014
		Residual	0.087 ± 0.014	0.044 ± 0.013	0.030 ± 0.013	0.023 ± 0.013
		Centroid	0.026 ± 0.013	0.030 ± 0.012	0.018 ± 0.013	0.030 ± 0.013
$\alpha = 0.9$	Normal	Bootstrap	0.029 ± 0.010	0.031 ± 0.011	0.021 ± 0.010	0.017 ± 0.010
		Bayesian	0.076 ± 0.012	0.054 ± 0.011	0.048 ± 0.011	0.045 ± 0.011
		Residual	0.043 ± 0.011	0.023 ± 0.010	0.025 ± 0.010	0.020 ± 0.010
		Centroid	0.027 ± 0.010	0.001 ± 0.009	0.012 ± 0.010	0.016 ± 0.010
	Percentile	Bootstrap	0.101 ± 0.013	0.036 ± 0.011	0.021 ± 0.010	0.014 ± 0.010
		Bayesian	0.129 ± 0.013	0.077 ± 0.012	0.059 ± 0.012	0.054 ± 0.011
		Residual	0.098 ± 0.013	0.030 ± 0.011	0.033 ± 0.011	0.025 ± 0.010
		Centroid	0.081 ± 0.012	0.021 ± 0.010	0.020 ± 0.010	0.015 ± 0.010
	Pivotal	Bootstrap	0.106 ± 0.013	0.045 ± 0.011	0.025 ± 0.010	0.023 ± 0.010
		Bayesian	0.149 ± 0.014	0.093 ± 0.012	0.073 ± 0.012	0.056 ± 0.011
		Residual	0.100 ± 0.013	0.044 ± 0.011	0.030 ± 0.011	0.023 ± 0.010
		Centroid	0.046 ± 0.011	0.013 ± 0.009	0.011 ± 0.010	0.020 ± 0.010
$\alpha = 0.95$	Normal	Bootstrap	0.018 ± 0.008	0.014 ± 0.008	0.012 ± 0.008	0.006 ± 0.007
		Bayesian	0.053 ± 0.010	0.038 ± 0.009	0.031 ± 0.009	0.037 ± 0.009
		Residual	0.036 ± 0.009	0.019 ± 0.008	0.011 ± 0.008	0.008 ± 0.007
		Centroid	0.018 ± 0.008	0.005 ± 0.006	0.009 ± 0.007	0.005 ± 0.007
	Percentile	Bootstrap	0.081 ± 0.010	0.047 ± 0.009	0.030 ± 0.008	0.017 ± 0.008
		Bayesian	0.126 ± 0.012	0.072 ± 0.010	0.056 ± 0.010	0.042 ± 0.009
		Residual	0.100 ± 0.011	0.040 ± 0.009	0.037 ± 0.009	0.021 ± 0.008
		Centroid	0.077 ± 0.010	0.029 ± 0.008	0.020 ± 0.008	0.016 ± 0.008
	Pivotal	Bootstrap	0.089 ± 0.011	0.043 ± 0.009	0.027 ± 0.008	0.015 ± 0.008
		Bayesian	0.127 ± 0.012	0.091 ± 0.011	0.064 ± 0.010	0.056 ± 0.010
		Residual	0.085 ± 0.011	0.051 ± 0.009	0.036 ± 0.009	0.029 ± 0.008
		Centroid	0.046 ± 0.009	0.002 ± 0.007	0.014 ± 0.008	0.009 ± 0.007

Table 3: Complete result on comparing centroid approximation with various bootstrap methods.

replacement. We consider the setting that we sample with replacement. These two schemes gives very similar result for vanilla bootstrap method. For the centroid approximation method, we generate 100 (i.e., $M = 100$) resampling (with replacement) copies and decide the u_w accordingly. We use RMSprop optimizer with learning rate 0.1. When making actions, we sample the prediction head according to $v_k^*(t)$ obtained using the examples between the last two model updates.

C.3 Centroid Approximation for Bootstrap DQN

More on Bootstrap DQN Similar to the bootstrap method in contextual bandit problem, Bootstrap DQN explores using the model uncertainty, which can be assessed via maintaining several models trained with bootstrapped training set. Maintaining several independent models can be very expensive in RL and to reduce the computational cost, Bootstrap DQN uses a multi-head network with a shared base. Each head in the network corresponds to a bootstrap model and the common shared base is thus trained via the union of the bootstrap training set of each head. We train the Bootstrap DQN with standard updating rule for DQN and use Double-DQN (Van Hasselt et al., 2016) to reduce the overestimate issue. Notice that our centroid approximation method only changes the memory buffer for each head and thus introduces no conflict to other possible techniques that can be applied to Bootstrap DQN.

More on experiment setup details We use a fully connected layer with 256 hidden neurons as the shared base and stack two fully connected layers each with 256 hidden neurons as head. For LunarLander-v2, we train the model for 450 episodes with the first 50 episodes used to initialize the memory buffer. The maximum number of steps within each episode is set to 1000. We report the moving average reward with window width 100. For Catcher-v0, we train the model for 100 episodes with the first 10 episodes used to initialize the memory buffer. We set the maximum number of steps within each episodes 2000 and report the moving average reward with window width 25.

For training the Bootstrap DQN, we update target model and the replay buffers for each head every 1000 steps for LunarLander-v2 and 200 steps for Catcher-v0. The policy network is updated every steps using one step gradient with Adam optimizer using 0.001 learning rate and 64 batch size. The update scheme for replay buffers is the same as the one in contextual bandit experiment and the max capacity is set to 50000 (the oldest data point will be pop out when size reaches maximum and new data comes in). For the shared base, following Osband et al. (2016), we adds up all the gradient comes from each head and normalizes it by the number of heads.

C.4 Bootstrap Ensemble Model

Ensemble of deep neural networks have been successfully used to boost predictive performance (Lakshminarayanan et al., 2016). In this experiment, we consider using an ensemble of deep neural network trained on different bootstrapped training set, which is also known as a popular strategy called *bagging*.

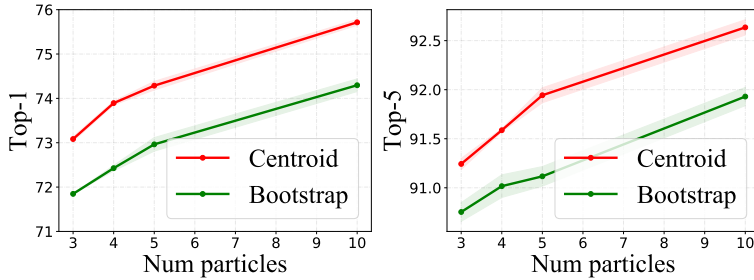


Figure 4: Results on ensemble modeling with bootstrap using Vgg16 on CIFAR-100.

#Particle	$\gamma = 0$	$\gamma = 0.5$	$\gamma = m$
3	3480.0 ± 120	3702.7 ± 89.8	3467.7 ± 115
4	3461.92 ± 126	3723.1 ± 78.7	3600.0 ± 69.3
5	3586.5 ± 64.5	3799.6 ± 84.2	3647.3 ± 64.5
10	3785.0 ± 59.1	3796.9 ± 36.1	3742.7 ± 86.8

Table 4: Ablation study.

We consider image classification task on CIFAR-100 and use standard VGG-16 (Simonyan and Zisserman, 2014) with batch normalization. We apply a standard training pipeline. We train the bootstrap model for 160 epochs using SGD optimizer with 0.9 momentum and batchsize 128. The learning rate is initialized to be 0.1 and is decayed by a factor of 10 at epoch 80 and 120. We start to apply the centroid approximation at epoch 120 (thus the centroid is initialized with 120 epochs’ training). We generate the bootstrap training set for each centroid every epoch using the proposed centroid approximation method. We consider $m = 3, 4, 5, 10$ ensembles and use $\gamma = 0.5/m$. We repeat the experiment for 3 random trials and report the averaged top1 and top5 accuracy with the standard deviation of the mean estimator.

Figure 4 summarizes the result. Overall, increasing m is able to improve the predictive performance and with the same number of models, our centroid approximation consistently improves over standard bootstrap ensembles.

C.5 Ablation Study

We study the effectiveness of using (8) to modify the gradient of centroid with $v_k^*(t) \leq \gamma$. We consider the setting $\gamma = 0$ (no modification) and $\gamma = m$ (always modify, equivalent to no bootstrap uncertainty) and applied the method on the mushroom dataset in the contextual bandit problem. Table 4 shows that (i) modifying the gradient of centroid with small $v_k^*(t)$ using do improve the overall result; (2) bootstrap uncertainty is important for exploration.

C.6 Computation overhead

Our main goal is not to decrease the training cost but improve the quality of bootstrap partial distribution so that we can use less models at deployment and hence reduce the memory cost and the computational cost for inference. Actually, as discussed in Section 3, our method actually only introduces a little computation overhead while much improves the quality of the particles, which is another advantage of our method. For example, in bandit problem on mushroom dataset, when $m = 3, 10$, vanilla bootstrap takes $33s, 101s$ while our approach takes $35s, 108s$ per run. For the bagging, when $m = 3, 10$, vanilla bootstrap takes $11200s, 34240s$ while ours take $12000s, 36200s$. Results are based on the average of 3 runs. Our method only introduces about 7% computational overhead even with an naive implementation.